SCIENTIFIC REPORTS

OPEN

SUBJECT AREAS:
PROTEOMIC ANALYSIS
BIOANALYTICAL CHEMISTRY
DIAGNOSTIC MARKERS

Received
4 April 2014

Accepted
28 July 2014

Published
3 September 2014

Correspondence and requests for materials should be addressed to W.E.H. (weh.scholar@gmail.com) or T.G.F. (thomas.forsthuber@utsa.edu)

Microwave & Magnetic (M^2) Proteomics Reveals CNS-Specific Protein Expression Waves that Precede Clinical Symptoms of Experimental Autoimmune Encephalomyelitis

Itay Raphael[1], Swetha Mahesula[1], Anjali Purkar[1], David Black[1], Alexis Catala[1], Jonathon A. L. Gelfond[2], Thomas G. Forsthuber[1] & William E. Haskins[1]

[1]University of Texas at San Antonio, San Antonio, TX 78249, [2]University of Texas Health Science Center at San Antonio, San Antonio, TX 78229.

Central nervous system-specific proteins (CSPs), transported across the damaged blood-brain-barrier (BBB) to cerebrospinal fluid (CSF) and blood (serum), might be promising diagnostic, prognostic and predictive protein biomarkers of disease in individual multiple sclerosis (MS) patients because they are not expected to be present at appreciable levels in the circulation of healthy subjects. We hypothesized that microwave & magnetic (M^2) proteomics of CSPs in brain tissue might be an effective means to prioritize putative CSP biomarkers for future immunoassays in serum. To test this hypothesis, we used M^2 proteomics to longitudinally assess CSP expression in brain tissue from mice during experimental autoimmune encephalomyelitis (EAE), a mouse model of MS. Confirmation of central nervous system (CNS)-infiltrating inflammatory cell response and CSP expression in serum was achieved with cytokine ELISPOT and ELISA immunoassays, respectively, for selected CSPs. M^2 proteomics (and ELISA) revealed characteristic CSP expression waves, including synapsin-1 and α-II-spectrin, which peaked at day 7 in brain tissue (and serum) and preceded clinical EAE symptoms that began at day 10 and peaked at day 20. Moreover, M^2 proteomics supports the concept that relatively few CNS-infiltrating inflammatory cells can have a disproportionally large impact on CSP expression prior to clinical manifestation of EAE.

Multiple sclerosis (MS) is a debilitating neurological disease that affects approximately 2.5 million people globally[1]. MS patients experience episodes of inflammation and demyelination that are believed to be mediated by an autoimmune attack directed against central nervous system (CNS)-specific proteins (CSPs) such as components of the myelin sheath on axons, including: myelin basic protein, proteolipid protein and myelin oligodendrocyte glycoprotein. The autoimmune attack promotes an inflammatory cascade in the CNS highlighted by recruitment of innate- and adaptive-immune cells and release of inflammatory mediators that act in concert to damage the myelin sheath and neuronal axons. Autoreactive T cells have been shown to be key mediators of this attack against the myelin sheath. Once activated, these T cells migrate and infiltrate into the CNS, crossing the blood-brain-barrier (BBB) in a multistep process[2,3]. Infiltrating autoreactive T cells release inflammatory cytokines that modulate the activation of microglia, infiltrating macrophages and dendritic cells to release neurotoxic mediators, including nitric oxide and reactive-oxygen species (ROS)[4,5]. Macrophages, microglia, and dendritic cells are also actively involved in the inflammatory response[6,7]. While MS research has historically focused on inflammatory events in the CNS, such as the pathological role of cytokines[8,9], a more detailed molecular understanding of the biology of other proteins, particularly CSPs transported across the BBB into cerebrospinal fluid (CSF) or serum, is critical to further our understanding of MS and to develop new biomarkers and treatments.

Clinical diagnosis of MS, versus other similar neurological diseases, and classification into the consensus definitions of the four major subtypes of MS is based on a limited diagnostic repertoire, including: clinical appearance, disease history and laboratory imaging and/or diagnostics[2,10–14]. Currently, MS is classified into relapsing-remitting (RRMS), secondary-progressive (SPMS), primary-progressive (PPMS) and progressive-

relapsing (PRMS). Approximately 80% of the patients initially develop the RRMS form of the disease, characterized by clinical attacks (relapses) with diverse neurological dysfunctions, followed by functional recovery (remission). More than half of these patients will eventually develop SPMS, characterized by progressive residual neurological deficiencies with or without attacks during the progressive phase[13]. Current immunomodulatory treatments ameliorate, but do not cure, MS, including: beta-interferons, therapeutic antibodies, glucocorticoids and glatiramer acetate. Responses to treatments are highly variable between patients and no accurate means exist to predict efficacy of a particular drug. Individual responses to treatment are typically evaluated by clinical measures of disease progression such as the expanded disability status scale (EDSS)[15] and magnetic resonance imaging (MRI) of brain lesion volume[16–19]. However, these clinical measures lack sensitivity and specificity for a large population of MS patients, and they fail to show a strong correlation between specific treatments and their efficacy in slowing disease progression in individual MS patients.

Thus, there is an urgent need for molecular biochemical markers with improved diagnostic, prognostic and predictive power. However, poorly understood variations of genetic, environmental, and socioeconomic factors in the MS patient population present profound challenges for biomarker research. A diagnostic matrix with a particular combination of biomarkers might enable more precise molecular stratification of individual patients into treatment groups. Moreover, a particular combination of biomarkers might be necessary because not all of these molecules are expected to be exclusive to MS and might also be found in other diseases and neurological disorders.

Studying the relation of protein expression trajectories to disease progression within individual MS patients is expected to mitigate population variability to a certain degree and account for potential patient-specific factors. More than 24,000 genes are translated and post-translationally modified into an estimated 2 million protein isoforms in humans, encoding far more molecular diversity than the relatively static genome or transcriptome. Paradoxically, less than 100 proteins are routinely quantified in serum today[20,21]. Thus, the most sensitive (most true-positive) and specific (least false-positive) biomarkers are expected to be at the protein level. Notably, proteins must be measured directly due to the poor correlation between the transcriptome and proteome due to alternative splicing, post-translational modifications, single nucleotide polymorphisms, limiting ribosomes available for translation, mRNA and protein stability, and other factors (e.g., microRNA).

CSPs, transported across the damaged BBB to CSF and blood (serum), might be promising diagnostic, prognostic and predictive (therapeutic) protein biomarkers of disease in individual MS patients because they are not expected to be present at appreciable levels in the circulation of healthy subjects. Compared to the highly variable clinical spectrum of individual MS patients, disease in groups of mice with experimental autoimmune encephalomyelitis (EAE), the major animal model for MS, is less heterogeneous and more synchronous, providing a strong rationale for preclinical biomarker studies. Our laboratory has pioneered microwave and magnetic (M^2) proteomics for quantitative liquid chromatography-tandem mass spectrometry (LC/MS/MS) of relatively large numbers of CSPs and brain tissue specimens in murine EAE[22,23]. M^2 proteomics synergizes off-line microwave-assisted chemical modification of CSPs bound to magnetic C8 microparticles, multiplexed isobaric encoding, and automated sample preparation with 96-well plates. M^2 proteomics is also amino acid sequence- and post-translational modification-specific[24–27]. Despite its advantages, LC/MS/MS-based proteomics of low abundance CSPs can be confounded by masking effects due to high abundance proteins, particularly in CSF and serum where protein abundance can span up to 12 orders of magnitude[28,29].

In this study, we hypothesized that M^2 proteomics of CSPs in brain tissue might be an effective means to prioritize putative CSP biomarkers for future immunoassays in CSF and serum, as previously suggested by us[22] and others[30]. To test this hypothesis, we longitudinally assessed CSP expression in brain tissue from EAE mice. Confirmation of autoimmune T-cell response and CSP expression trajectories was achieved with cytokine ELISPOT and ELISA immunoassays, respectively, for selected CSPs. Importantly, M^2 proteomics revealed characteristic CSP expression waves that preceded the onset of clinical EAE symptoms.

Results

The EAE score distribution and disease trajectory for mice that were blindly scored for clinical symptoms, including those randomly selected for analysis with M^2 proteomics, are shown in Figure 1. Consistent with previous reports including our own studies, only few mice exhibited mild clinical symptoms (EAE score $\leq$ 1) by day 7 (pre-onset), with increased EAE scores evident for disease onset at day 10 (EAE score $\geq$ 1) and disease peak at day 20 (EAE score $\geq$ 2), followed by decreased EAE scores for remission at day 25[31–33].

Next, we tested for expression changes in the CNS proteome in order to prioritize CSPs that might be promising biomarkers of EAE. We focused on analysis of the brain-tissue proteome because the brain is the major target of the disease in MS[34–36]. Overall, decoding isobarically-labeled peptide expression for each specimen relative to pooled reference materials enabled statistical calculations for 1032 peptides from CSPs and other putative protein biomarkers (from a total of 6608 peptides and 4512 proteins) with significant differential expression between two post-immunization time points (pair-wise time point contrasts) and significant differential expression across all post-immunization time points (overall p-value). Specifically, we required top-scoring peptides to have pair-wise time point contrast with an area under the receiver operating characteristic curve (AUC) greater than 0.9 and an overall p-value of less than 1.0E-03, respectively.

Importantly, M^2 proteomics revealed characteristic CSP expression waves, including synapsin-1 and α-II-spectrin, which peaked at day 7 in brain tissue and preceded clinical EAE symptoms that began at day 10 and peaked at day 20. CSP expression waves that were consistently observed are shown in Supplementary Tables 1A&B and Supplementary Tables 2A&B, respectively.

Shown in Figure 2 is synapsin-1 as a representative example for the expression of CSPs over the course of disease. Of the 19 peptides that were observed from synapsin-1 across all time points, 17 showed a significant differential expression with peak levels at day 7 (5 representative peptides are shown in Figure 2). Five representative peptides from synapsin-1 with significant differential expression (pair-wise time point contrasts) between 5 vs. 7 days and between 0 vs. 7 days are shown in Figure 3. Here, for instance the AUC for peptide GSHSQSSSPGALTLGR (peptide 2 of 19) for day 5 vs. day 7 was 0.99 and 0.95 for reference material tagged with the TMT126 and TMT131 isobaric labeling reagents, respectively (bold in Table 1). The overall p-values for this peptide were 8.1E-12 or 1.9E-08 for reference material chemically modified with the TMT126 and TMT131 isobaric labeling reagents, respectively. Correlations of relative peptide expression to post-immunization time were superior to correlations to EAE score (8.8E-01 and 4.4E-01, respectively). The remaining 2 of 19 peptides (QASISGPAPTK and QGPPQKPPGPAGPTR) were outliers, with AUC values less than 0.9 for pair-wise time point contrasts that included day 7 (e.g., day 0 vs. day 7).

Compared to our previous work[22], a five-fold larger cohort and two different pooled reference materials (TMT-126 and -131-labeled) were selected to improve the statistical power of and confidence in our results for a number of putative protein biomarkers. In addition, CSPs and other putative protein biomarkers for MS

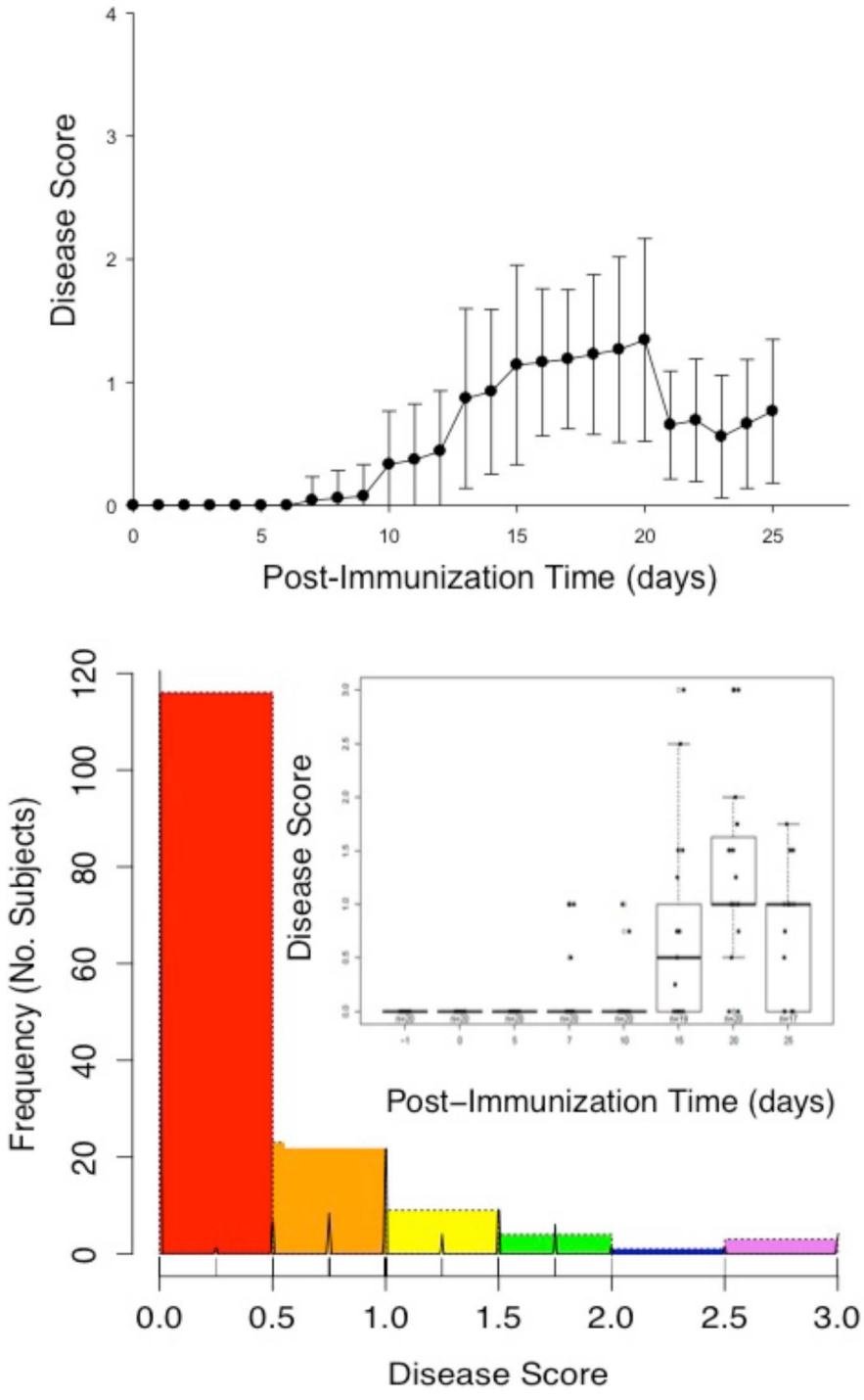

Figure 1 | Disease trajectory for the entire cohort studied herein (top), where mice were evaluated daily for EAE clinical symptoms. The disease distribution and disease trajectory for the mice for M^2 proteomics are also shown (bottom and inset, respectively). Mice for M^2 proteomics were randomly selected and sacrificed from 8 disease time points ($18 \leq n \leq 20$ specimens per time point), described by the number of days (d) post-immunization [−1 d (non-immunized), 0 d (3 hrs post-immunization), 5 d, 7 d, 10 d, 15 d, 20 d and 25 d]. These time points were selected to reflect inflection points of pre-onset, disease onset, early disease, disease peak and remission.

patients were prioritized and selected from our dataset by excluding non-CSPs with descriptive terms for the protein name found in the Trembl protein database. Consequently, we observed approximately four-fold more peptides (and CSPs) than previously reported by applying the more stringent constraints described above (e.g., overall p-values less than 5.0E-02; AUC calculation). Statistical correlations of peptide expression to EAE score and post-immunization time were also improved and resulted in the identification of new putative CSP biomarkers, including: synapsin-1 and α-II-spectrin. In addition, the overall p-value previously reported for the peptide LIETYFSK from proteolipid protein 1 improved from 8.0E-04 ([22]) to 7.9E-12 with the TMT126-labeled reference material (Supplementary Tables 2A&B). Additional confidence in this result was provided by the TMT131-labeled reference material (overall p-value = 4.7E-

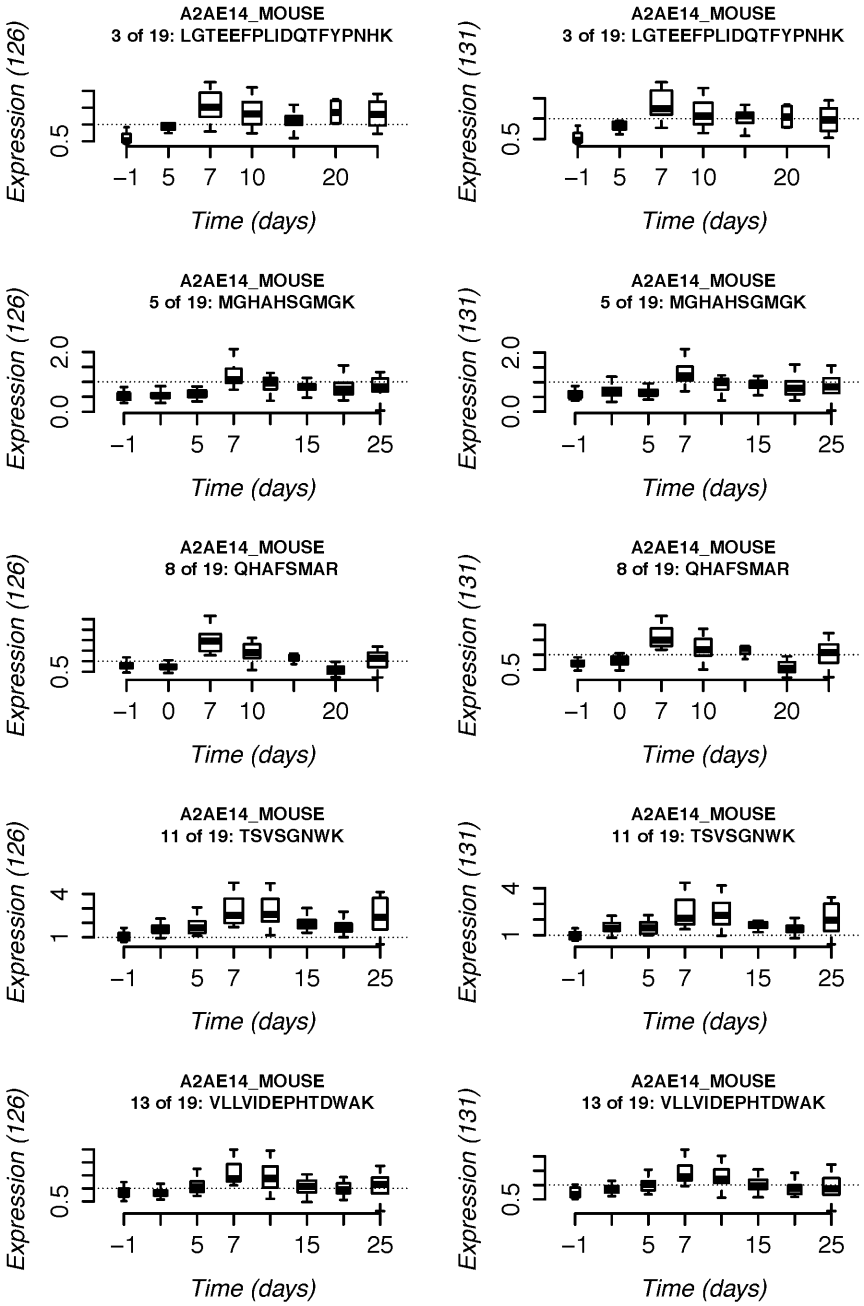

Figure 2 | M² proteomics trajectories for selected differentially expressed peptides from synapsin-1 (A2AE14_MOUSE). Values for 1) significant differential expression (AUC > 0.9) between two post-immunization time points and 2) significant differential expression (overall p-value < 1.0E-03) across all post-immunization time points are provided in Supplementary Information.

12). Similar results were obtained for the peptide GLSATVTGGQK from proteolipid protein 1. Lastly, AUC values greater than 0.9 were observed for both peptides (Supplementary Tables 1A&B).

In addition to synapsin-1 and α-II-spectrin, differentially expressed CSPs and other proteins included: synapsin-2/3, myelin basic protein, ubiquitin carboxyl-terminal esterase L1, calcium/calmodulin-dependent protein kinase II alpha, neurofilament light and medium, park 2, peroxiredoxin-1/4/5/6, 14-3-3-β/ε/ζ, synaptotagmin, enolase-1/2, guanine nucleotide binding protein α and β1, superoxide dismutase 2, internexin neuronal intermediate filament protein α, tyrosine-protein phosphatase non-receptor type substrate 1, macrophage migration inhibitory factor, proteolipid protein 1, and caspase 7 (a brief description of several of these proteins is provided in Supplementary Text).

CSP expression waves, revealed with M² proteomics of brain tissue, were confirmed with ELISAs of representative CSPs in serum specimens from an independent cohort (Figure 4). Synapsin-1 and α-II-spectrin were selected because of their statistical significance. Serum was collected, pooled and analyzed with ELISAs from mice with EAE scores similar to the EAE scores of mice at the specific post-immunization time points that were analyzed with M² proteomics. A strong correlation between the levels of synapsin-1 and α-II-spectrin in brain tissue and serum was observed, with peak levels at day 7 (Figure 4).

To provide a better understanding of the mechanism underlying the characteristic CSP expression waves we investigated CNS-infiltrating inflammatory cell responses by immunoassays over the course of EAE. Cytokine ELISPOT assays showed that neuroantigen-react-

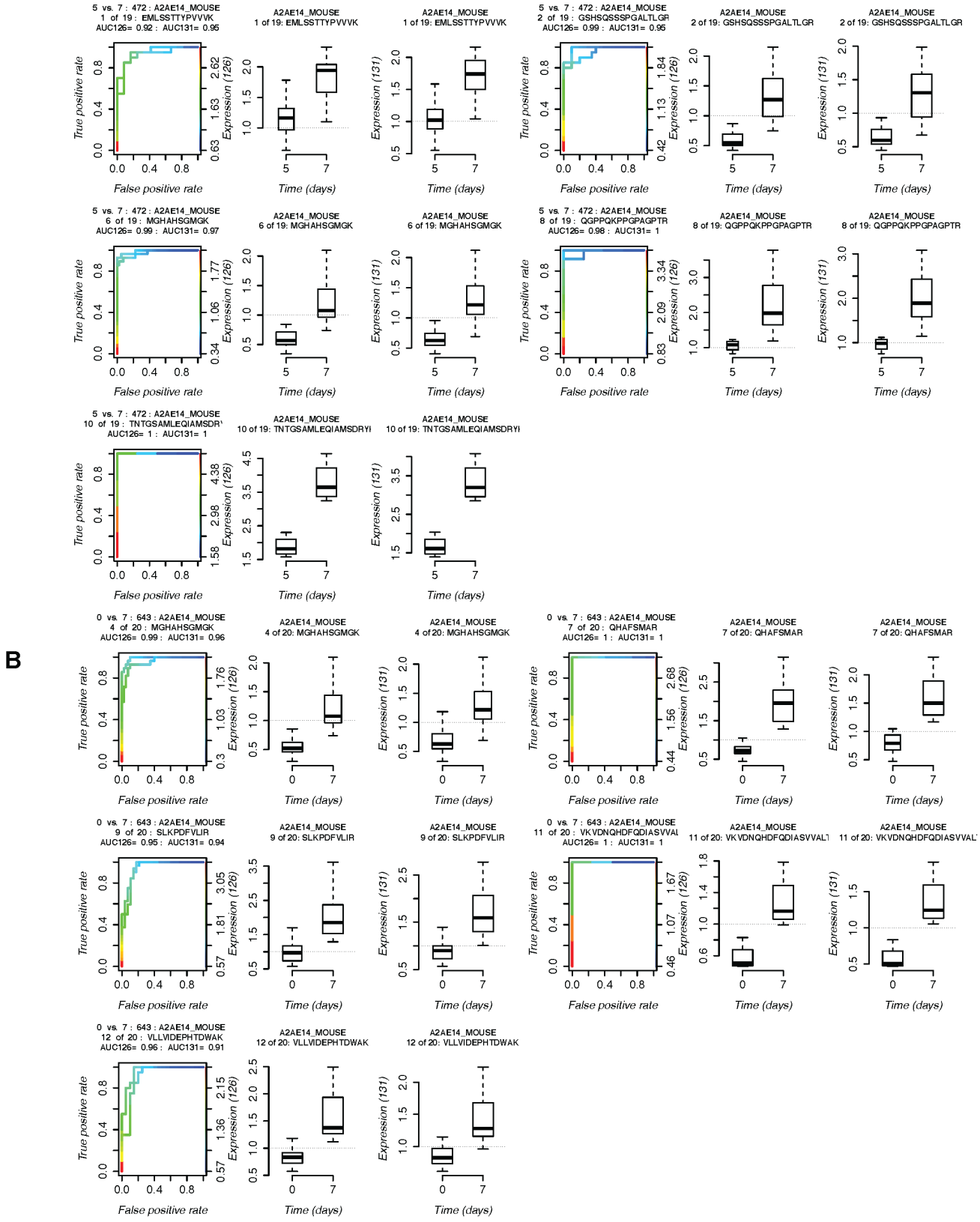

Figure 3 | Synapsin-1 (A2AE14_MOUSE) yielded A) 5 peptides with significant differential expression (pair-wise time point contrasts) between 5 vs. 7 days and (B) 5 peptides with significant differential expression between 0 vs. 7 days post-immunization.

ive T cells producing two well-studied pathogenic cytokines (IFN-γ and IL-17) could be detected in spleen tissue as early as day 5 after disease induction, and T cell responses peaked by day 15 (Figure 5). In contrast, notable neuroantigen-specific T cell responses could be detected in the brain only by day 10, coinciding with the onset of EAE. Consistent with our previous findings, the frequencies of cytokine-producing T cells in brain tissue peaked by day 20, coinciding with peak EAE disease scores[22,23]. Importantly, the frequencies of

Table 1 | Synapsin 1 (A2AE14_MOUSE) peptides with an AUC greater than 0.9

Post-immunization time contrast (e.g., day 0 vs. day 7)		Peptide Sequence	AUC126	AUC131	Overall p-value 126	Overall p-value 131
−1	5	VKVDNQHDFQDIASVVALTK	1.00	1.00	5.0E-09	1.9E-13
−1	7	LGTEEFPLIDQTFYPNHK	0.98	0.98	3.6E-05	9.5E-04
−1	7	MGHAHSGMGK	1.00	0.99	1.6E-25	5.9E-22
−1	7	QHAFSMAR	1.00	1.00	1.3E-19	4.1E-14
−1	7	TSVSGNWK	1.00	0.99	1.7E-10	1.7E-09
−1	7	VKVDNQHDFQDIASVVALTK	1.00	1.00	5.0E-09	1.9E-13
−1	7	VLLVIDEPHTDWAK	0.98	0.99	5.9E-14	4.6E-13
−1	10	KLGTEEFPLIDQTFYPNHK	0.94	0.96	3.6E-04	1.4E-06
−1	10	LGTEEFPLIDQTFYPNHK	0.98	0.94	3.6E-05	9.5E-04
−1	10	QHAFSMAR	0.90	0.92	1.3E-19	4.1E-14
−1	10	TSVSGNWK	0.98	0.96	1.7E-10	1.7E-09
−1	10	VKVDNQHDFQDIASVVALTK	1.00	1.00	5.0E-09	1.9E-13
−1	15	LGTEEFPLIDQTFYPNHK	0.94	0.97	3.6E-05	9.5E-04
−1	15	MGHAHSGMGK	0.94	0.95	1.6E-25	5.9E-22
−1	15	QHAFSMAR	0.93	0.96	1.3E-19	4.1E-14
−1	15	TSVSGNWK	0.95	0.95	1.7E-10	1.7E-09
−1	20	VKVDNQHDFQDIASVVALTK	0.96	1.00	5.0E-09	1.9E-13
0	7	MGHAHSGMGK	0.99	0.96	1.6E-25	5.9E-22
0	7	QHAFSMAR	1.00	1.00	1.3E-19	4.1E-14
0	7	SLKPDFVLIR	0.95	0.94	1.6E-11	5.0E-10
0	7	VKVDNQHDFQDIASVVALTK	1.00	1.00	5.0E-09	1.9E-13
0	7	VLLVIDEPHTDWAK	0.96	0.91	5.9E-14	4.6E-13
5	7	EMLSSTTYPVVVK	0.92	0.95	1.7E-07	1.6E-03
5	**7**	**GSHSQSSSPGALTLGR**	**0.99**	**0.95**	**8.1E-12**	**1.9E-08**
5	7	MGHAHSGMGK	0.99	0.98	1.6E-25	5.9E-22

neuroantigen-reactive T cells in brain tissue were negligible on day 7, consistent with the very low number of inflammatory cells detectable in the CNS at this time point (data not shown; Sosa *et al*[33]). In agreement with the notion that very few inflammatory cells were present in the CNS by day 7 after induction of disease, and consistent with the cytokine ELISPOT results (Figure 5), M^2 proteomics showed that CD4 expression (a representative marker of CNS-infiltrating T cells) increased with the onset of disease at day 10 and peaked in brain tissue by day 20 (Supplementary Figure 1).

Overall, the results showed a disproportional relationship between the significant changes in CSP expression detected at day 7 and the very low number of CNS-infiltrating inflammatory cell responses at this time point. Since the magnitude of the peripheral (e.g. spleen or blood) neuroantigen-specific immune response was not correlated to EAE onset or severity, the results suggest that CSPs may be more sensitive biomarkers for inflammatory demyelinating CNS disease than inflammatory biomarkers such as cytokines. Moreover, CSPs are also expected to be more specific biomarkers for early detection of EAE because they are not expected at appreciable levels in healthy controls, whereas neuroantigen-specific immune responses can be detected in healthy individuals[37,38].

Stratification of risk groups was further investigated with non-supervised and supervised hierarchical clustering of relative peptide expression and/or post-immunization time. Non-supervised hierarchical clustering did not accurately stratify subjects by post-immunization time. However, many nearest neighbor misclassifications, where subjects were incorrectly grouped adjacent to one another rather than one group removed from one another, were observed across all top-ranked proteins (Figure 6A). In other words, misclassifications between day −1 and day 0 or between day 10 and day15 were observed more often than misclassifications between day −1 and day 7 or between day 10 and day 20. In contrast, supervised hierarchical clustering of all top-ranked proteins recapitulated our AUC calculations. Along these lines, supervised hierarchical clustering showed that peak levels of 17 of 19 peptides from synapsin-1 clustered at day 7 (selected peptides shown in Figure 6B). Furthermore, visual inspection revealed the same two outliers (QASISGPAPTK and QGPPQKPPGPAGPTR) that were observed in our AUC calculations. Overall, these results suggest that M^2 proteomics classifiers might be constructed to stratify risk groups based on post-immunization time.

Pathway and network analysis showed enrichment of differentially expressed CSPs and other proteins in specific signaling pathways and molecular networks. For example, P-values for enrichment of the top-ranked molecular network entitled "neurological disease and motor dysfunction" in the Ingenuity knowledgebase were most significant at day 7, coinciding with characteristic CSP expression waves (Figure 7). Enrichment of other key pathways that might be important to MS patients, such as the 14-3-3 signaling pathway[22,23], were also observed to peak at day 7.

Discussion

In this report, we investigated whether M^2 proteomics of brain tissue might be an effective means to prioritize putative CSP biomarkers for future immunoassays in CSF and serum, by measuring changes in the brain during the disease as previously suggested by us[22] and others[30,39]. First, we showed that M^2 proteomics of CSPs in brain tissue revealed characteristic CSP expression waves that preceded the onset of clinical EAE symptoms. Second, we confirmed the CNS-infiltrating inflammatory cell response and CSP expression trajectories in serum with cytokine ELISPOT and ELISA immunoassays, respectively, for selected CSPs found to have significant expression changes prior to clinical onset. Based on our results M^2 proteomics of CSPs in brain tissue is an effective means to prioritize putative CSP biomarkers for future immunoassays in serum and/or other body fluids (e.g., CSF).

To the best of our knowledge, CNS-specific protein expression waves that precede clinical symptoms of EAE have not been described previously. However, CSPs have been previously suggested as promising biomarkers for MS, and CSPs have been previously observed to be differentially expressed in CNS tissue, CSF and blood from EAE models and MS patients[40]. EAE is a mainstay in the field for studying brain inflammation and the mechanisms involved in MS

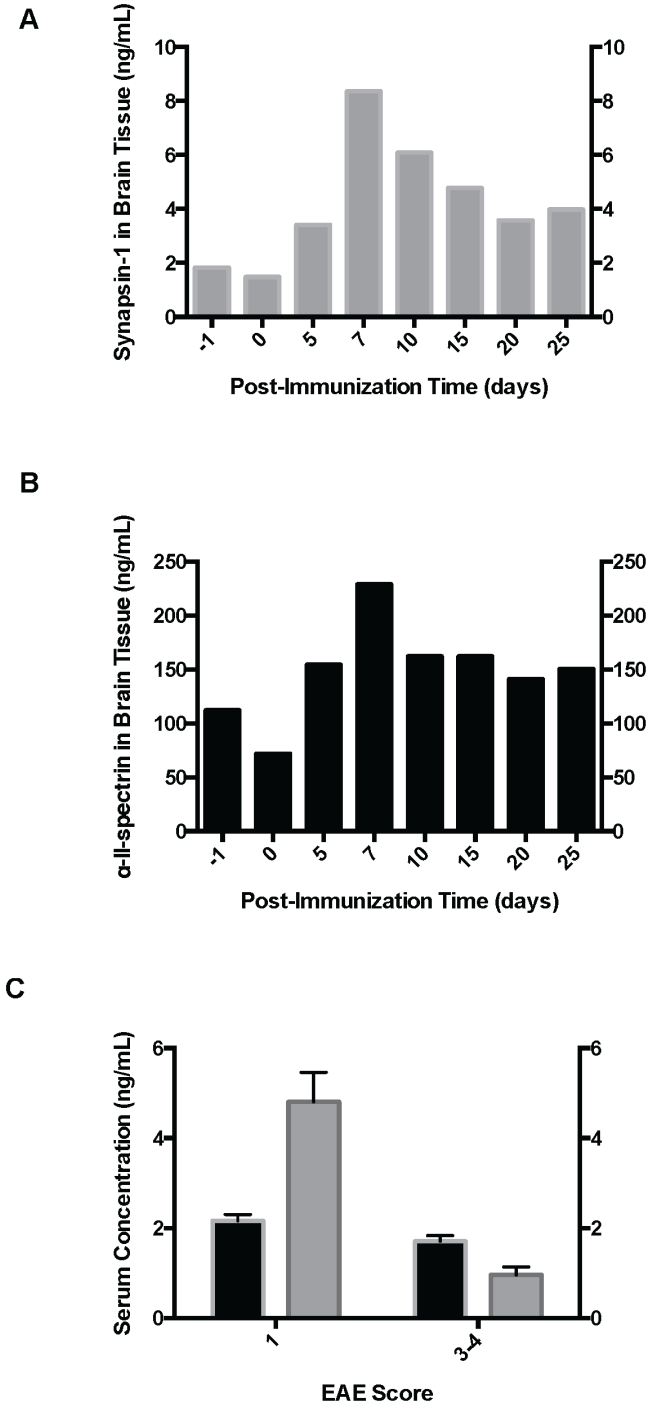

Figure 4 | ELISA results for levels of two CSPs: (A) synapsin-1 in brain tissue, (B) α-II-spectrin in brain tissue, and (C) synapsin-1 (gray) and α-II-spectrin (black) in serum (n=5, avg±sd).

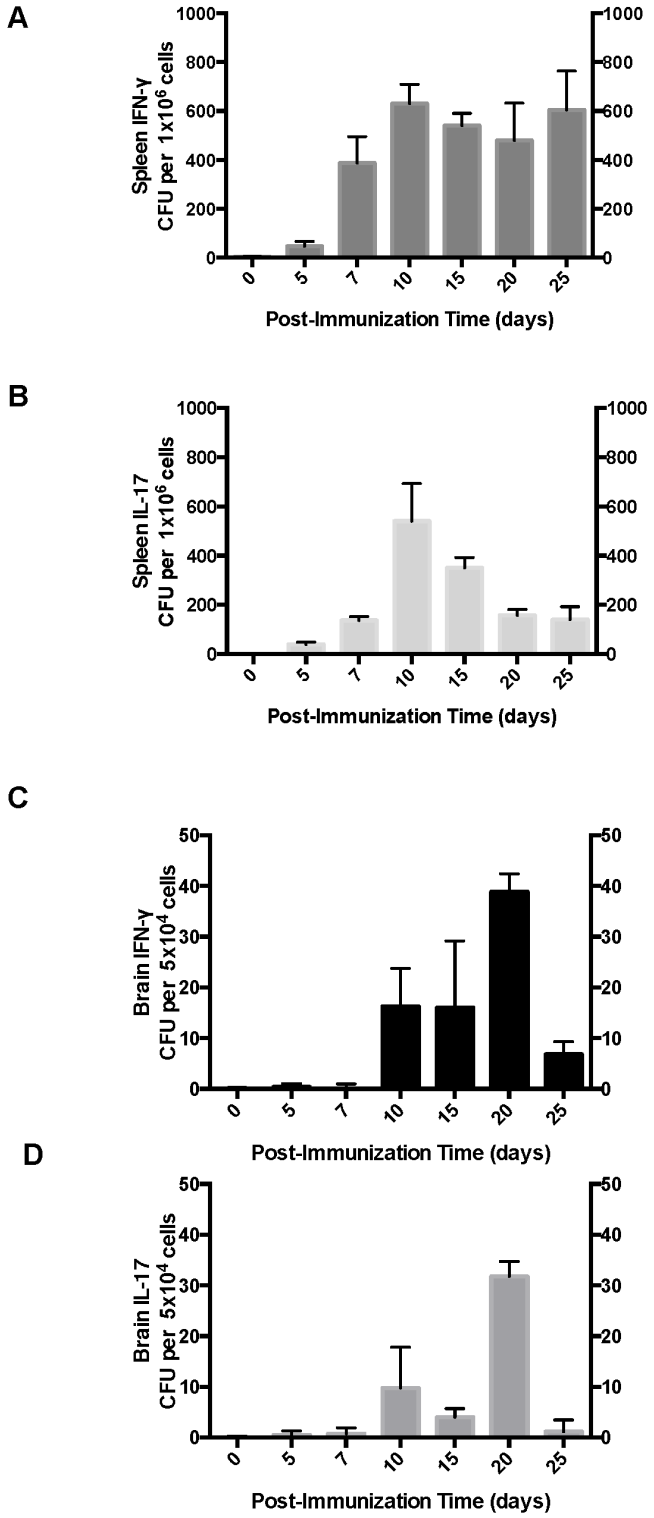

Figure 5 | ELISPOT results for levels of two pro-inflammatory cytokines: (A) IFN-γ in spleen tissue, (B) IL-17 in spleen tissue, (C) IFN-γ in brain tissue, and (D) IL-17 in brain tissue.

pathology because it closely mimics disease progression in RRMS patients[30,40–42].

CNS-infiltrating inflammatory cell responses that disrupt the permeability of the BBB, including the secretion of ROS and matrix metalloproteinases (MMPs), can partially explain the differential expression (transport) of CSPs in circulation[43]. Our results suggest that the CSP wave observed on day 7 is likely the result of the initiation of the autoimmune attack on the CNS by an early wave of autoimmune T-cells and other inflammatory cells infiltrating the CNS during the course of EAE. Evidence for the former comes from previous work showing that cytokine production by autoreactive CD4+ T cells in the CNS is concomitant with EAE score measures of clinical symptoms[22,23]. Furthermore, while investigating the kinetics of myelin antigen uptake by APCs in the CNS during EAE, we detected a significant increase in the uptake of myelin antigen by day 7[33], which coincides with the appearance of CSP expression waves at day 7 as shown herein (including synapsin-1 and α-II-spectrin).

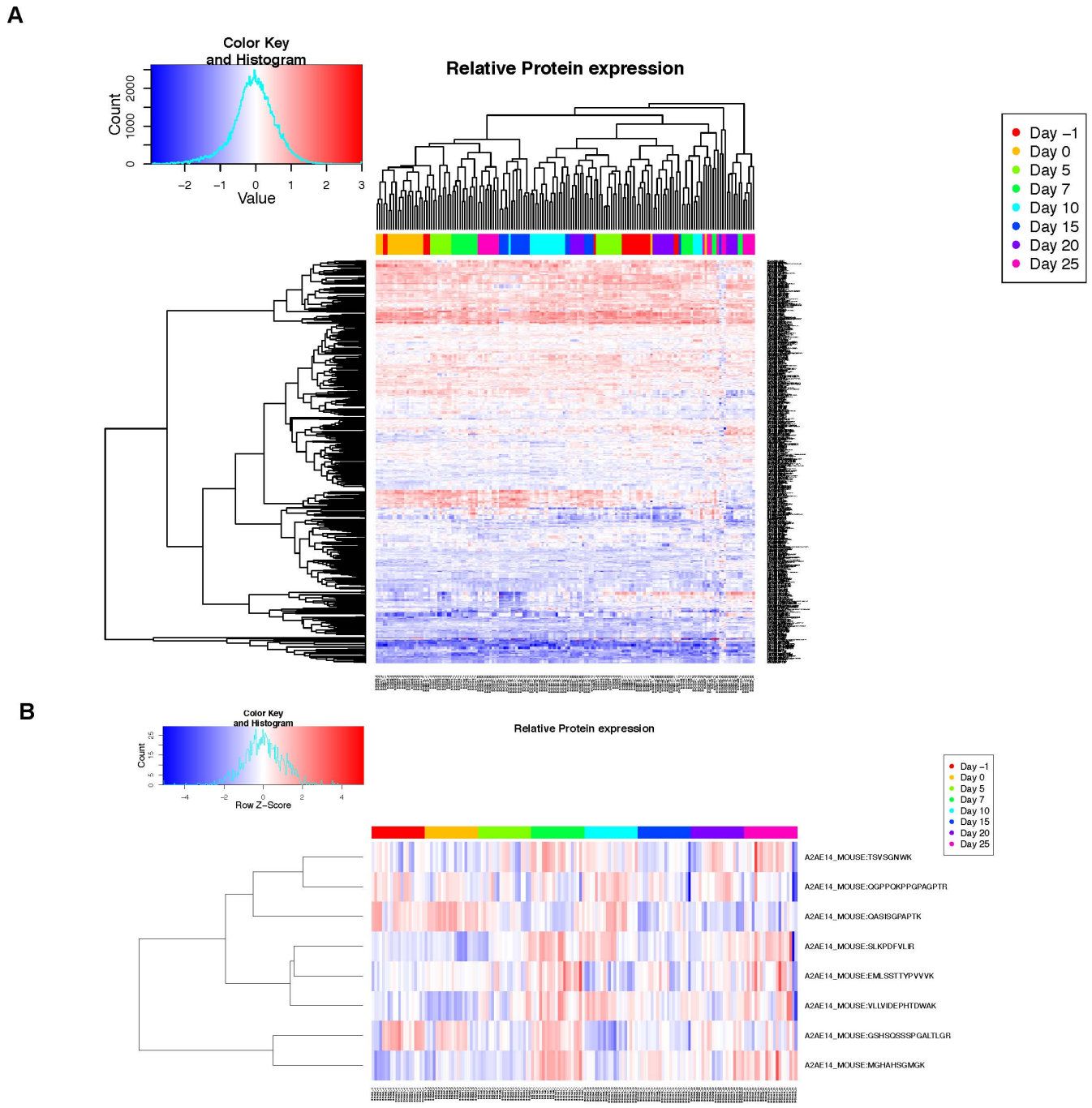

Figure 6 | Hierarchical clustering of risk groups by correlating relative peptide expression to post-immunization time for a subset of CSPs and other putative protein biomarkers measured by M² proteomics. (A) shows non-supervised clustering for all CSPs, while (B) shows representative supervised hierarchical clustering results for synapsin-1 (A2AE14_MOUSE).

Thus, the results suggest that a relatively small number of inflammatory cells entering the CNS during the initiation of the disease process in EAE (and possibly MS) can cause major changes in the CNS proteome detectable by M² proteomics. Our results further suggest that at least some of the CSPs can be detected in serum and could potentially be useful as biomarkers for EAE disease. Identification of similar markers in MS patients could have major diagnostic, prognostic and predictive (therapeutic) implications.

Synapsin-1, one of the CSPs reported in this study, is a phosphorylated CSP found at synaptic vesicles in neurons which can bind to several cytoskeleton components including actin, microtubules and α-II-spectrin[44–46]. It is involved in synaptogenesis and calcium-dependent neurotransmitter release from synaptic vesicles, particularly glutamate release[47]. To the best of our knowledge, synapsin-1 has not yet been implicated in pathogenesis of MS, albeit the disruption of synapsin-1 mediated-exocytosis may lead to glutamate neurotoxicity and other symptoms observed in patients with MS or other neuro-degenerative/-inflammatory diseases[48,49]. Previous work in EAE showed that early inflammation enhanced glutamate release and promoted synaptic degeneration and dendritic spine loss in a demyelination-independent manner[50]. Additionally, proteins that are involved in glutamate metabolism and toxicity, including glutamate dehydrogenase 1 mitochondrial and glutamine sythnetase, were reported to be regulated in EAE or MS[40].

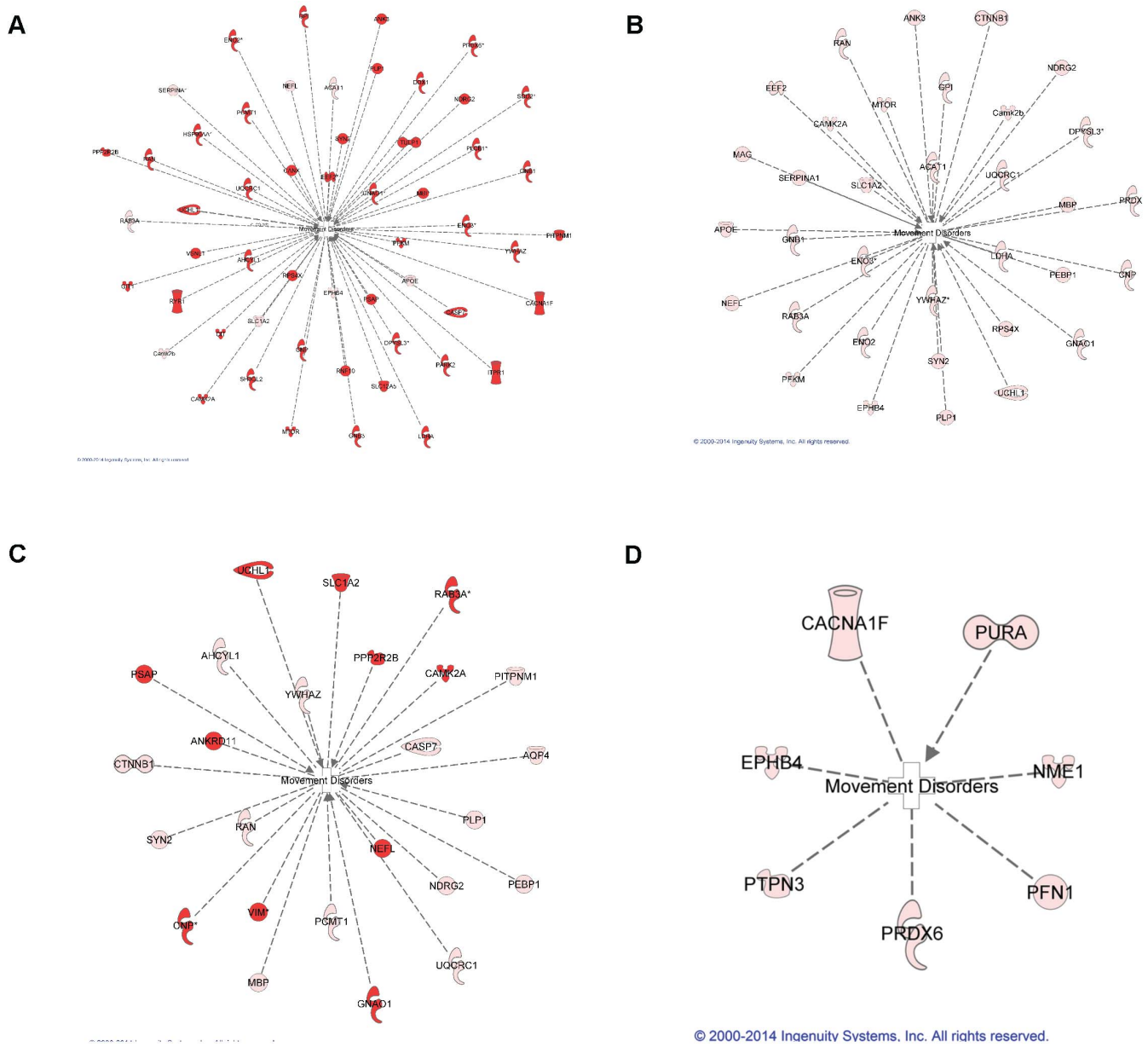

Figure 7 | Enrichment of CSPs and other putative protein biomarkers in specific pathways, including a molecular network for neurological disease and motor dysfunction, as a function of post-immunization time. P-values for enrichment of this network were most significant (A) prior to clinical manifestation of disease onset ($p = 4.02E-17$ for days 0 and −1 vs. 5 and 7), followed by (B) disease onset ($p = 4.12E-11$ for days 0 and −1 vs. 10), (C) the peak of disease ($p = 9.89E-09$ for days 0 and −1 vs. 10 and 15) and (D) remission ($p = 3.95E-04$ for days 0 and −1 vs. 25).

The spectrin-family is comprised of a group of membrane-bound proteins, including α-II-spectrin, that are present in most vertebrate tissues and were initially discovered as a component of erythrocyte membrane[51,52]. Spectrin is composed of two subunits, α and β, that coil around each other to form a heterodimer[53]. The α subunit is encoded by two different genes, while the β subunit is encoded by five different genes: alternative splicing generates additional isoforms (reviewed in[54–57]). In the CNS, almost all major cell types express spectrin, with distinct isoforms found in different cell types[54,58–63]. α-II-spectrin is predominantly localized to axons and to presynaptic terminals of neurons[64–67] with an essential role in Ca+ mediated exocytosis and neurotransmitter release through its association with synapsin proteins that are found in the neuronal vesicles[54]. α-II-spectrin is also cleaved by calcium-dependent cysteine proteases such as calpains and caspases during necrosis and apoptosis to generate breakdown products that are often protease-specific[68–70]. Indeed, the breakdown products of α-II-spectrin in CSF have been shown to be potential biomarkers of traumatic brain injury[71–75].

Importantly, both calpain and caspase were found to be differentially expressed either during EAE or MS, and were suggested to be potential biomarkers for these diseases[40]. Here we reported that a downstream substrate of these enzymes, α-II-spectrin, as well as an upstream protein that is involved in glutamate toxicity, synapsin-1, are differentially expressed during EAE both in the CNS and serum. Hence both these proteins could potentially be biomarkers for EAE (and MS).

Our observation of characteristic CSP waves highlights the subtle changes in CSP expression trajectories that can be observed with M^2 proteomics. This is largely due to improved statistical power ($18 \leq n \leq 20$ specimens × 8 time-points) that could be difficult or impossible to achieve by other methods. Indeed, previous proteomics studies of EAE and MS brain tissue have suffered from poor sample

throughput due to lengthy sample preparation times, particularly when fractionation and/or immunodepletion steps are incorporated to minimize masking effects. Consequently, those studies have been statistically underpowered, focusing on qualitative or semi-quantitative methods for identifying large numbers of proteins in relatively small numbers of specimens and time-points.

Previously we reported that changes in the level of glucose-6-phosphate isomerase and several other proteins (e.g., 14-3-3ε, proteolipid protein 1; peroxiredoxin 1, etc.) mirror disease progression in EAE[22]. We also quantified myelin basic protein, macrophage migration inhibitory factor, and CD47[23]. Some of these proteins were also reported to be regulated during MS and/or EAE[40]. A number of proteins that we detected in our current study were also reported by others, including actins, tubulins, enolases, glial fibrillary acidic protein (GFAP) and neurofilaments etc[40]. However, to develop useful candidate biomarkers we focused on CSPs because they are not expected at appreciable levels in the circulation of healthy subjects. Thus, ubiquitous cytoskeletal proteins such as tubulins did not meet our inclusion criteria.

While many CSPs were revealed herein, differential expression of several well-studied CSPs was not statistically significant. For example, GFAP did not meet the inclusion criteria because it had low AUC values and high overall p-values. Future work is needed to improve the penetrance and confidence of M^2 proteomics and other proteomics strategies for low abundance CSPs, particularly for serum studies. Masking of low abundance CSPs such as GFAP by higher abundance proteins may explain why an expression trajectory might not be statistically significant. We have shown that masking can be partially overcome by immunoenrichment of low abundance proteins prior to M^2 proteomics[23], and immunodepletion of high abundance proteins is another potentially viable option. However, masking of CSPs is problematic for serum specimens[76,77]. For these reasons and others, we suggest that M^2 proteomics of CSP expression waves in brain tissue is an effective means to prioritize putative CSP biomarkers for future immunoassays in CSF and serum. Moreover, discovering CSP expression waves in EAE with M^2 proteomics is expected to provide critical information that might not be revealed by other MS studies, including biomarkers that are predictive of disease onset, severity, chronic progression and response to treatment.

Lastly, the characteristic CSP expression waves revealed by our studies need to be investigated in prospective longitudinal studies in serum from individual mice for their usefulness as predictors of disease onset, severity and/or disease progression. Furthermore, these waves will need to be investigated as potential markers for treatment efficacy and development of treatment resistance, i.e. to glucocorticoid treatment. If successful, these studies can provide a framework for individualized treatment of patients.

We anticipate that a particular combination of characteristic CSP expression waves with high sensitivity and selectivity, for which at least some are expected to be observable independent of clinical measures of disease progression (EDSS or MRI), will be helpful to personalize and improve MS diagnostics and treatment. To achieve this, preclinical studies that assess CSP waves in individual subjects with clinical symptoms and treatment conditions over the course of disease are needed. While additional studies are needed, M^2 proteomics supports the concept that relatively few CNS-infiltrating inflammatory cells can have a disproportionally large impact on CSP expression prior to clinical manifestation of EAE.

Methods

Murine experimental autoimmune encephalomyelitis (EAE). All animals were maintained in pathogen free conditions in the American Association for Laboratory Animal Science (AALAS) facility at the University of Texas at San Antonio. All experiments were approved by the Institutional Animal Care and Use Committee (IACUC) and performed in accordance with the relevant guidelines and regulations.

Five week-old C57BL/6 female mice were purchased from the Jackson Laboratory (Stock number 000664; Bar Harbor, ME) and used at 6–8 weeks of age in the studies. Mice were allowed to rest for 8 days before commencing the studies. Active induction of EAE was performed with a subcutaneous injection of each mouse with 200 μg of myelin oligodendrocyte glycoprotein (MOG) 35–55 peptide (United Biochemical Research, Seattle, WA) in 50 μL of complete Freund's adjuvant (CFA) containing Mycobacterium tuberculosis H37Ra (Difco Laboratories, Detroit, MI) at a final concentration of 5 mg/mL. Two intra-peritoneal (i.p.) injections of *Bordetella pertussis* toxin (PTX; List Biological, Campbell, CA) at 200 ng per mouse were given at the time of immunization and 48 hours later[78]. Animals were monitored and graded daily for clinical signs of EAE using the following scoring system[79]: 0, no abnormality; 1, limp tail; 2, moderate and hind limb weakness; 3, complete hind limb paralysis; 4, quadriplegia or premoribund state; 5, death. Mice for M^2 proteomics were randomly selected and sacrificed at 8 disease time points, described by the number of days (d) post-immunization [−1 d (non-immunized), 0 d (3 hrs post-immunization), 5 d, 7 d, 10 d, 15 d, 20 d and 25 d] ($n \sim 20$ per time point). These time points were selected to reflect inflection points of pre-onset, disease onset, early disease, disease peak and remission. These time points are a practical compromise between the minimum number of mice and the minimum number of samples required to define the overall trajectory of disease progression. Brain tissue was snap-frozen in liquid nitrogen and stored at −80°C until further use by cytokine immunoassays and M^2 proteomics.

Cytokine immunoassays. Antigen-induced T cell responses were assessed in dissociated brain and spleen tissue by enzyme-linked immunosorbent spot (ELISPOT) assay for interferon-γ and interleukin-17A (IFN-γ and IL-17) as previously described[80] after stimulation with MOG35-55 peptide (United Biochemical Research, Seattle, WA). Briefly, ELISPOT plates (Multiscreen IP; Millipore) were coated with anti-IFN-γ (AN-18; 1 μg/mL) or anti-IL-17A (17F3; 2 μg/mL) capture antibodies in phosphate buffered saline (PBS). The plates were blocked with 1% bovine serum albumin (BSA) in PBS for 1 h at room temperature and then washed four times with PBS. After 1 hour of blocking with PBS/1%BSA, cells were added with or without antigen and incubated for 24 h at 37°C. The plates were washed three times with PBS and four times with PBS/Tween 20, and biotinylated anti-IFN-γ (R4-6A2; 0.5 μg/ml) or IL-17A (eBioTC11-8H4; 0.125 μg/ml) detection antibodies were added and incubated overnight, respectively. Plates were washed four times with PBS/Tween 20 and incubated with streptavidin-alkaline phosphatase (Invitrogen). Cytokine spots were visualized with a BCIP/NBT phosphatase substrate (Kirkegaard & Perry Laboratories, Gaithersburg, MD). Image analysis of ELISPOT assays was performed with a Series 6 Universal-V Immunospot analyzer and Immunospot 5.1 software (Cellular Technology Limited) as described previously[81,82]. Results for antigen-specific T cells were normalized with a negative control containing peptide-free media. All measurements were performed in duplicate.

Brain tissue lysate. Whole cell protein was extracted from brain tissue using the RIPA Lysis Buffer Kit (Santa Cruz Biotechnology, Inc. Santa Cruz, CA.) according to the manufacturer's protocol. Briefly, an appropriate amount of RIPA complete lysis buffer was added to cell pellet. The mixture was incubated on ice for 5 minutes, followed by centrifugation at 14000× g for 15 min at 4°C. The supernatant was collected as brain tissue lysate and stored at −80°C until further use. Protein concentration was determined using Invitrogen EZQ Protein Quantitation Kit (Invitrogen, Grand Island, NY). Protein from all mice ($n = 157$), spanning all time points, was pooled as reference material.

Microwave & magnetic (M^2) sample preparation. *For isobaric TMT labeling*, protein was pooled from all specimens by protein amount as reference material prior to sample preparation from individual specimens. Approximately 50 mg of C8 magnetic beads (BcMg, Bioclone Inc.) were suspended in 1 mL of 50% methanol. Immediately before use, 100 μL of the beads were washed 3 times with equilibration buffer (200 mM NaCl, 0.1% trifluoroacetic acid (TFA)). Whole cell protein lysate (25–100 μg at 1 μg/μL) was mixed with pre-equilibrated beads and 1/3rd sample binding buffer (800 mM NaCl, 0.4% TFA) by volume. The mixture was incubated at room temperature for 5 min followed by removing the supernatant. The beads were washed twice with 150 μL of 40 mM triethylammonium bicarbonate (TEAB), and then 150 μL of 10 mM dithiolthreitol (DTT) was added. The bead-lysate mixture underwent microwave heating for 10 s. DTT was removed and 150 μL of 50 mM iodoacetamide (IAA) added, followed by a second microwave heating for 10 s. The beads were washed twice and re-suspended in 150 μL of 40 mM TEAB. *In vitro* proteolysis was performed with 4 μL of trypsin in a 1 : 25 trypsin-to-protein ratio (stock = 1 μg/μL in 50 mM acetic acid) and microwave heated for 20 s in triplicate. The supernatant was used immediately or stored at −80°C. Released tryptic peptides from digested protein lysates, including the reference materials described above, were modified at the N-terminus and at lysine residues with the tandem mass tagging (TMT)-6plex isobaric labeling reagents (Thermo scientific, San Jose, CA). Each individual specimen was encoded with one of the TMT-127-130 reagents, while reference material was encoded with the TMT-126 and -131 reagents: 41 μL of anhydrous acetonitrile was added to 0.8 mg of TMT labeling reagent for 25 μg of protein lysate and microwave-heated for 10 s. To quench the reaction, 8 μL of 5% hydroxylamine was added to the sample at room temperature. To normalize across all specimens, TMT-encoded cell lysates from individual specimens, labeled with the TMT-127-130 reagents, were mixed with the reference material encoded with the

TMT-126 and -131 reagents in $1_{126}:1_{127}:1_{128}:1_{129}:1_{130}:1_{131}$ ratios. These sample mixtures, including all TMT-encoded specimens, were stored at −80°C until further use.

Capillary liquid chromatography-fourier-transform-tandem mass spectrometry (LC/FT/MS/MS) with protein database searching. Capillary LC/FT/MS/MS was performed with a splitless nanoLC-2D pump (Eksigent, Livermore, CA), a 50 μm-i.d. column packed with 7 cm of 3 μm-o.d. C18 particles, and a hybrid linear ion trap-Fourier-transform tandem mass spectrometer (LTQ-ELITE; ThermoFisher, San Jose, CA) operated with a lock mass for calibration. The reverse-phase gradient was 2 to 62% of 0.1% formic acid (FA) in acetonitrile over 60 min at 350 nL/min. *For unbiased analyses*, the top 6 most abundant eluting ions were fragmented by data-dependent HCD with a mass resolution of 120,000 for MS and 15,000 for MS/MS. *For isobaric TMT labeling*, probability-based protein database searching of MS/MS spectra against the Trembl protein database (release 2012_dec29; 59,862 sequences) was performed with a 10-node MASCOT cluster (v. 2.3.02, Matrix Science, London, UK) with the following search criteria: peak picking with Mascot Distiller; 10 ppm precursor ion mass tolerance, 0.8 Da product ion mass tolerance, 3 missed cleavages, trypsin, carbamidomethyl cysteines as a static modification, oxidized methionines and deamidated asparagines as variable modifications, an ion score threshold of 20 and TMT-6-plex for quantification.

ELISA immunoassays. Commercial ELISA Kits for α-II-spectrin (SEA292Mu) and synapsin-1 (SEC883Mu) were used per the manufacturer's suggested protocol (USCN Life Science Inc), where 500 μg of protein pooled from each time point (n ~ 20 per group) was added to the corresponding well in each plate. Plates were read at OD 450 nm for absorbance on a Synergy HT microplate reader (BioTek). For serum specimens, serum was collected from mice with mild EAE disease (disease score = 1; day 10) or severe disease (score = 3–4; day 20) and 1,500 μg of pooled serum samples were analyzed in triplicate with 4–5 mice per pool.

Prioritization of CSPs and other putative protein biomarkers. CSPs and other putative protein biomarkers for MS patients were selected from our dataset by excluding proteins with the following descriptive terms for the protein name found in the Trembl protein database: heat shock, tubulin, histone, albumin, globin, lysosomal, mitochondrial, actin, dehydrogenase, myosin, transferrin, fructokinase, fructose, citrate, cytochrome c, glutathione, microtubule, ATP, clathrin, centromere, NADH, centrosomal, non-neuronal, elongation factor, peroxisomal, annexin, hexokinase, pyruvate, ribosomal, nucleoside, cofilin, titin, transcriptional inhibitory, initiation factor, glutamine, dynamin, RNA, cytoskeleton-associated, transducin, growth factor, vacuolar, tumor-related, phosphorylase, ribonucleoprotein, peptidyl-prolyl cis-trans isomerase, CoA, excision repair, phosphatase, zinc finger, triosephosphate isomerase, adenylyl, and keratin.

Statistical analysis. The M^2 proteomics results for each technical replicate estimate peptide expression for individual mice, encoded in sample mixtures, relative to pooled reference material from all mice, spanning all time points. Relative peptide expression levels were transformed to log base 2 for quantile normalization. Outlier arrays were removed based upon the following quality control procedures: 1) overall intensity histograms of normalized expression were compared with kernel smoothed density plots, and 2) hierarchical clustering of sample profiles was performed to assess the consistency of technical and biological variation. We tested the association between relative peptide expression and EAE score using a linear mixed-effect while treating EAE score as a continuous predictor. First, we treated the EAE effect on relative peptide expression singly, as a univariate predictor. Next, we considered the effects of EAE score by adjusting for time as a quadratic effect. We tested for changes in relative peptide expression with post-immunization time using a linear mixed-effect model in which time was a treated as a multilevel factor. We tested all the pairwise differences in relative peptide expression between all disease time points, including both non-immunized mice (day −1) and 3 hrs post-immunization (day 0), using an unpaired, unequal variance t-test on the replicate averages. We examined the relationship between the overall peptide expression profile with time or EAE score using a hierarchical clustering display based upon Euclidean distance and complete linkage. For clustering analyses of relative peptide expression profiles, we considered the subset of peptides that were most variable by selecting the peptides in the top quartile (top 25%) by their standard deviation ranking. Finally, we investigated the area under the receiver operating characteristic curve (AUC) for top-scoring peptides (AUC > 0.9) from CSPs and other putative protein biomarkers, prioritized from our dataset as described above[83], and compared these values with overall p –values. Proteins were selected only if at least one peptide met the following inclusion criteria: 1) significant differential expression (AUC > 0.9) between two post-immunization time points and 2) significant differential expression (overall p-value < 1.0E-03) across all post-immunization time points. All statistical analysis was performed with R v3.0.2 (R-Project, Vienna, Austria).

Pathway and network analysis. Pathway and network analysis was performed with Ingenuity Pathways Analysis (IPA, Ingenuity R Systems) according to the manufacturer's suggestions. Briefly, MASCOT results were imported to IPA as .csv files and IPA's core analysis was performed on each file. Differentially expressed proteins corresponding to genes in the IPA knowledgebase were mapped onto canonical signaling pathways and molecular networks per the manufacturer's recommendations. A vertical bar plot, showing the percentage of proteins quantified in each canonical signaling pathway, was visualized to investigate pathway and molecular network enrichment during disease progression, where p-values for enrichment were assigned by IPA.

1. Mateen, F. J. *et al.* Neurological disorders in the 11th revision of the International Classification of Diseases: now open to public feedback. *Lancet Neurol* **11**, 484–485, doi:10.1016/S1474-4422(12)70125-4 (2012).
2. Steinman, L. Multiple sclerosis: a coordinated immunological attack against myelin in the central nervous system. *Cell* **85**, 299–302 (1996).
3. Goverman, J. Autoimmune T cell responses in the central nervous system. *Nat Rev Immunol* **9**, 393–407, doi:10.1038/nri2550 (2009).
4. Rovaris, M. *et al.* Secondary progressive multiple sclerosis: current knowledge and future challenges. *Lancet Neurol* **5**, 343–354, doi:10.1016/S1474-4422(06)70410-0 (2006).
5. Dhib-Jalbut, S. *et al.* Neurodegeneration and neuroprotection in multiple sclerosis and other neurodegenerative diseases. *J Neuroimmunol* **176**, 198–215 (2006).
6. Hartung, H. P. *et al.* Inflammatory mediators in demyelinating disorders of the CNS and PNS. *J Neuroimmunol* **40**, 197–210 (1992).
7. Benveniste, E. N. Role of macrophages/microglia in multiple sclerosis and experimental allergic encephalomyelitis. *J Mol Med (Berl)* **75**, 165–173 (1997).
8. Veldhoen, M. The role of T helper subsets in autoimmunity and allergy. *Curr Opin Immunol* **21**, 606–611, doi:10.1016/j.coi.2009.07.009 (2009).
9. Olsson, T. Cytokines in neuroinflammatory disease: role of myelin autoreactive T cell production of interferon-gamma. *J Neuroimmunol* **40**, 211–218 (1992).
10. Sospedra, M. & Martin, R. Immunology of multiple sclerosis. *Annu Rev Immunol* **23**, 683–747, doi:10.1146/annurev.immunol.23.021704.115707 (2005).
11. Noseworthy, J. H., Lucchinetti, C., Rodriguez, M. & Weinshenker, B. G. Multiple sclerosis. *N Engl J Med* **343**, 938–952, doi:10.1056/NEJM200009283431307 (2000).
12. Thompson, A. J. *et al.* Primary progressive multiple sclerosis. *Brain: a journal of neurology* **120 (Pt 6)**, 1085–1096 (1997).
13. Lublin, F. D. & Reingold, S. C. Defining the clinical course of multiple sclerosis: results of an international survey. National Multiple Sclerosis Society (USA) Advisory Committee on Clinical Trials of New Agents in Multiple Sclerosis. *Neurology* **46**, 907–911 (1996).
14. Confavreux, C., Vukusic, S., Moreau, T. & Adeleine, P. Relapses and progression of disability in multiple sclerosis. *NEJM* **343**, 1430–1438, doi:10.1056/NEJM200011163432001 (2000).
15. Poonawalla, A. H. *et al.* Composite MRI scores improve correlation with EDSS in multiple sclerosis. *Mult Scler* **16**, 1117–1125, doi:10.1177/1352458510374892 (2010).
16. Bakshi, R. *et al.* MRI in multiple sclerosis: current status and future prospects. *Lancet Neurol* **7**, 615–625, doi:10.1016/S1474-4422(08)70137-6 (2008).
17. Tourdias, T. & Dousset, V. Neuroinflammatory Imaging Biomarkers: Relevance to Multiple Sclerosis and its Therapy. *Neurotherapeutics*, doi:10.1007/s13311-012-0155-4 (2012).
18. Filippi, M. & Agosta, F. Imaging biomarkers in multiple sclerosis. *J Magn Reson Imaging* **31**, 770–788, doi:10.1002/jmri.22102 (2010).
19. Neema, M., Stankiewicz, J., Arora, A., Guss, Z. D. & Bakshi, R. MRI in multiple sclerosis: what's inside the toolbox? *Neurotherapeutics* **4**, 602–617, doi:10.1016/j.nurt.2007.08.001 (2007).
20. Rifai, N., Gillette, M. A. & Carr, S. A. Protein biomarker discovery and validation: the long and uncertain path to clinical utility. *Nat Biotechnol* **24**, 971–983 (2006).
21. Anderson, N. L. & Anderson, N. G. The human plasma proteome: history, character, and diagnostic prospects. *Mol Cell Proteomics* **1**, 845–867 (2002).
22. Raphael, I. *et al.* Microwave and magnetic (M(2)) proteomics of the experimental autoimmune encephalomyelitis animal model of multiple sclerosis. *Electrophoresis* **33**, 3810–3819, doi:10.1002/elps.201200200 (2012).
23. Mahesula, S. *et al.* Immunoenrichment microwave and magnetic proteomics for quantifying CD47 in the experimental autoimmune encephalomyelitis model of multiple sclerosis. *Electrophoresis* **33**, 3820–3829, doi:10.1002/elps.201200515 (2012).
24. Ottens, A. K. *et al.* Neuroproteomics in neurotrauma. *Mass Spec Rev* **25**, 380–408, doi:10.1002/mas.20073 (2006).
25. Ottens, A. K. *et al.* A multidimensional differential proteomic platform using dual-phase ion-exchange chromatography-polyacrylamide gel electrophoresis/reversed-phase liquid chromatography tandem mass spectrometry. *Anal Chem* **77**, 4836–4845, doi:10.1021/ac050478r (2005).
26. Haskins, W. E. *et al.* Rapid discovery of putative protein biomarkers of traumatic brain injury by SDS-PAGE-capillary liquid chromatography-tandem mass spectrometry. *J Neurotrauma* **22**, 629–644, doi:10.1089/neu.2005.22.629 (2005).
27. Wang, K. K. *et al.* Proteomics studies of traumatic brain injury. *Intl Rev Neurobiology* **61**, 215–240, doi:10.1016/S0074-7742(04)61009-9 (2004).
28. Kushnir, M. M. *et al.* Measurement of thyroglobulin by liquid chromatography-tandem mass spectrometry in serum and plasma in the presence of antithyroglobulin autoantibodies. *Clin Chem* **59**, 982–990, doi:10.1373/clinchem.2012.195594 (2013).
29. Lehmann, S. *et al.* Quantitative Clinical Chemistry Proteomics (qCCP) using mass spectrometry: general characteristics and application. *Clin Chem Lab Med: CCLM/FESCC* **51**, 919–935, doi:10.1515/cclm-2012-0723 (2013).

30. Robinson, W. H., Utz, P. J. & Steinman, L. Genomic and proteomic analysis of multiple sclerosis. Opinion. *Curr Opin Immunol* **15**, 660–667 (2003).
31. Shen, P. *et al.* IL-35-producing B cells are critical regulators of immunity during autoimmune and infectious diseases. *Nature* **507**, 366–370, doi:10.1038/nature12979 (2014).
32. Sriskantharajah, S. *et al.* Regulation of experimental autoimmune encephalomyelitis by TPL-2 kinase. *J Immunol* **192**, 3518–3529, doi:10.4049/jimmunol.1300172 (2014).
33. Sosa, R. A., Murphey, C., Ji, N., Cardona, A. E. & Forsthuber, T. G. The kinetics of myelin antigen uptake by myeloid cells in the central nervous system during experimental autoimmune encephalomyelitis. *J Immunol* **191**, 5848–5857, doi:10.4049/jimmunol.1300771 (2013).
34. Peterson, J. W., Bo, L., Mork, S., Chang, A. & Trapp, B. D. Transected neurites, apoptotic neurons, and reduced inflammation in cortical multiple sclerosis lesions. *Ann Neurology* **50**, 389–400 (2001).
35. Klaver, R., De Vries, H. E., Schenk, G. J. & Geurts, J. J. Grey matter damage in multiple sclerosis: a pathology perspective. *Prion* **7**, 66–75, doi:10.4161/pri.23499 (2013).
36. Lassmann, H. The pathology of multiple sclerosis and its evolution. *Phil Trans R Soc B* **354**, 1635–1640, doi:10.1098/rstb.1999.0508 (1999).
37. Encinas, J. A. *et al.* Genetic analysis of susceptibility to experimental autoimmune encephalomyelitis in a cross between SJL/J and B10.S mice. *J Immunol* **157**, 2186–2192 (1996).
38. Bahmanyar, S., Moreau-Dubois, M. C., Brown, P., Cathala, F. & Gajdusek, D. C. Serum antibodies to neurofilament antigens in patients with neurological and other diseases and in healthy controls. *J Neuroimmunol* **5**, 191–196 (1983).
39. Hu, J. *et al.* Optimized proteomic analysis of a mouse model of cerebellar dysfunction using amine-specific isobaric tags. *Proteomics* **6**, 4321–4334, doi:10.1002/pmic.200600026 (2006).
40. Farias, A. S., Pradella, F., Schmitt, A., Santos, L. M. & Martins-de-Souza, D. Ten years of proteomics in multiple sclerosis. *Proteomics* **14**, 467–480, doi:10.1002/pmic.201300268 (2014).
41. Han, M. H. *et al.* Janus-like opposing roles of CD47 in autoimmune brain inflammation in humans and mice. *J Exp Med* **209**, 1325–1334, doi:10.1084/jem.20101974 (2012).
42. Fallarino, F. *et al.* Metabotropic glutamate receptor-4 modulates adaptive immunity and restrains neuroinflammation. *Nat Med* **16**, 897–902, doi:10.1038/nm.2183 (2010).
43. Spindler, K. R. & Hsu, T. H. Viral disruption of the blood-brain barrier. *Trends Microbiol* **20**, 282–290, doi:10.1016/j.tim.2012.03.009 (2012).
44. Petrucci, T. C. & Morrow, J. S. Synapsin I: an actin-bundling protein under phosphorylation control. *J Cell Biol* **105**, 1355–1363 (1987).
45. Baines, A. J. & Bennett, V. Synapsin I is a microtubule-bundling protein. *Nature* **319**, 145–147, doi:10.1038/319145a0 (1986).
46. Sikorski, A. F., Terlecki, G., Zagon, I. S. & Goodman, S. R. Synapsin I-mediated interaction of brain spectrin with synaptic vesicles. *J Cell Biol* **114**, 313–318 (1991).
47. Nichols, R. A., Sihra, T. S., Czernik, A. J., Nairn, A. C. & Greengard, P. Calcium/calmodulin-dependent protein kinase II increases glutamate and noradrenaline release from synaptosomes. *Nature* **343**, 647–651, doi:10.1038/343647a0 (1990).
48. Choi, D. W. Glutamate neurotoxicity and diseases of the nervous system. *Neuron* **1**, 623–634 (1988).
49. Choi, D. W. Glutamate neurotoxicity in cortical cell culture is calcium dependent. *Neurosci Lett* **58**, 293–297 (1985).
50. Centonze, D. *et al.* Inflammation triggers synaptic alteration and degeneration in experimental autoimmune encephalomyelitis. *J Neurosci* **29**, 3442–3452, doi:10.1523/JNEUROSCI.5804-08.2009 (2009).
51. Marchesi, V. T. & Steers, E., Jr. Selective solubilization of a protein component of the red cell membrane. *Science* **159**, 203–204 (1968).
52. Repasky, E. A., Granger, B. L. & Lazarides, E. Widespread occurrence of avian spectrin in nonerythroid cells. *Cell* **29**, 821–833 (1982).
53. Speicher, D. W. & Marchesi, V. T. Erythrocyte spectrin is comprised of many homologous triple helical segments. *Nature* **311**, 177–180 (1984).
54. Goodman, S. R. *et al.* Brain spectrin: of mice and men. *Brain research bulletin* **36**, 593–606 (1995).
55. Stankewich, M. C. *et al.* A widely expressed betaIII spectrin associated with Golgi and cytoplasmic vesicles. *Proc Natl Acad Sci U.S.A.* **95**, 14158–14163 (1998).
56. Berghs, S. *et al.* betaIV spectrin, a new spectrin localized at axon initial segments and nodes of ranvier in the central and peripheral nervous system. *J Cell Biol* **151**, 985–1002 (2000).
57. Stabach, P. R. & Morrow, J. S. Identification and characterization of beta V spectrin, a mammalian ortholog of Drosophila beta H spectrin. *J Biol Chem* **275**, 21385–21395, doi:10.1074/jbc.C000159200 (2000).
58. Goodman, S. R. *et al.* A spectrin-like protein from mouse brain membranes: immunological and structural correlations with erythrocyte spectrin. *Cell Mot* **3**, 635–647 (1983).
59. Goodman, S. R. *et al.* A spectrin-like protein from mouse brain membranes: phosphorylation of the 235,000-dalton subunit. *Am J Phys* **247**, C61–73 (1984).
60. Goodman, S. R., Lopresti, L. L., Riederer, B. M., Sikorski, A. & Zagon, I. S. Brain spectrin(240/235A): a novel astrocyte specific spectrin isoform. *Brain Res Bulletin* **23**, 311–316 (1989).
61. Goodman, S. R., Zagon, I. S., Coleman, D. B. & McLaughlin, P. J. Spectrin expression in neuroblastoma cells. *Brain Res Bulletin* **16**, 597–602 (1986).
62. Zagon, I. S., McLaughlin, P. J. & Goodman, S. R. Localization of spectrin in mammalian brain. *J Neurosci* **4**, 3089–3100 (1984).
63. Clark, M. B. *et al.* Brain alpha erythroid spectrin: identification, compartmentalization, and beta spectrin associations. *Brain Res* **663**, 223–236 (1994).
64. DeBello, W. M., Betz, H. & Augustine, G. J. Synaptotagmin and neurotransmitter release. *Cell* **74**, 947–950 (1993).
65. Riederer, B. M., Zagon, I. S. & Goodman, S. R. Brain spectrin(240/235) and brain spectrin(240/235E): two distinct spectrin subtypes with different locations within mammalian neural cells. *J Cell Biol* **102**, 2088–2097 (1986).
66. Riederer, B. M., Lopresti, L. L., Krebs, K. E., Zagon, I. S. & Goodman, S. R. Brain spectrin(240/235) and brain spectrin(240/235E): conservation of structure and location within mammalian neural tissue. *Brain Res Bull* **21**, 607–616 (1988).
67. Zagon, I. S., Higbee, R., Riederer, B. M. & Goodman, S. R. Spectrin subtypes in mammalian brain: an immunoelectron microscopic study. *J Neurosci* **6**, 2977–2986 (1986).
68. Wang, K. K. *et al.* Simultaneous degradation of alphaII- and betaII-spectrin by caspase 3 (CPP32) in apoptotic cells. *J Biol Chem* **273**, 22490–22497 (1998).
69. Siman, R., Baudry, M. & Lynch, G. Brain fodrin: substrate for calpain I, an endogenous calcium-activated protease. *Proc Natl Acad Sci U.S.A.* **81**, 3572–3576 (1984).
70. Harris, A. S., Croall, D. E. & Morrow, J. S. The calmodulin-binding site in alpha-fodrin is near the calcium-dependent protease-I cleavage site. *J Biol Chem* **263**, 15754–15761 (1988).
71. Pineda, J. A. *et al.* Clinical significance of alphaII-spectrin breakdown products in cerebrospinal fluid after severe traumatic brain injury. *J Neurotrauma* **24**, 354–366, doi:10.1089/neu.2006.003789 (2007).
72. Cardali, S. & Maugeri, R. Detection of alphaII-spectrin and breakdown products in humans after severe traumatic brain injury. *J Neurosurg Sci* **50**, 25–31 (2006).
73. Hall, E. D. *et al.* Spatial and temporal characteristics of neurodegeneration after controlled cortical impact in mice: more than a focal brain injury. *J Neurotrauma* **22**, 252–265, doi:10.1089/neu.2005.22.252 (2005).
74. Beer, R. *et al.* Temporal profile and cell subtype distribution of activated caspase-3 following experimental traumatic brain injury. *J Neurochem* **75**, 1264–1273 (2000).
75. Weiss, E. S. *et al.* Alpha II-spectrin breakdown products serve as novel markers of brain injury severity in a canine model of hypothermic circulatory arrest. *Ann Thoracic Surg* **88**, 543–550, doi:10.1016/j.athoracsur.2009.04.016 (2009).
76. Jaros, J. A., Guest, P. C., Bahn, S. & Martins-de-Souza, D. Affinity depletion of plasma and serum for mass spectrometry-based proteome analysis. *Meth Molecular Biol* **1002**, 1–11, doi:10.1007/978-1-62703-360-2_1 (2013).
77. Koutroukides, T. A. *et al.* Characterization of the human serum depletome by label-free shotgun proteomics. *J Sep Sci* **34**, 1621–1626, doi:10.1002/jssc.201100060 (2011).
78. Munoz, J. J. & Mackay, I. R. Production of experimental allergic encephalomyelitis with the aid of pertussigen in mouse strains considered genetically resistant. *J Neuroimmunol* **7**, 91–96 (1984).
79. Nekrasova, T. *et al.* ERK1-deficient mice show normal T cell effector function and are highly susceptible to experimental autoimmune encephalomyelitis. *J Immunol* **175**, 2374–2380 (2005).
80. Shive, C. L., Hofstetter, H., Arredondo, L., Shaw, C. & Forsthuber, T. G. The enhanced antigen-specific production of cytokines induced by pertussis toxin is due to clonal expansion of T cells and not to altered effector functions of long-term memory cells. *Eur J Immunol* **30**, 2422–2431, doi:10.1002/1521-4141(2000)30:8<2422::AID-IMMU2422>3.0.CO;2-H (2000).
81. Heeger, P. S. *et al.* Revisiting tolerance induced by autoantigen in incomplete Freund's adjuvant. *J Immunol* **164**, 5771–5781 (2000).
82. Hofstetter, H. H. & Forsthuber, T. G. Kinetics of IL-17- and interferon-gamma-producing PLPp-specific CD4 T cells in EAE induced by coinjection of PLPp/IFA with pertussis toxin in SJL mice. *Neurosci Lett* **476**, 150–155, doi:10.1016/j.neulet.2010.04.018 (2010).
83. Sing, T., Sander, O., Beerenwinkel, N. & Lengauer, T. ROCR: visualizing classifier performance in R. *Bioinformatics* **21**, 3940–3941, doi:10.1093/bioinformatics/bti623 (2005).

Acknowledgments

This project was supported by National Institute of Health grants G12MD007591 (WEH, TGF), grants NS52177 and NS084201 (TGF), NIH5U54RR022762-05 (WEH), grant RG5011 from the National Multiple Sclerosis Society (TGF), and a fellowship of the South Texas Center for Emerging Infectious Diseases (IR). We thank the RCMI program and facilities at UTSA for assistance. The authors also acknowledge the support of the Cancer Therapy and Research Center at the University of Texas Health Science Center San Antonio, a National Cancer Institute -designated Cancer Center (NIHP30CA054174).

Author contributions

I.R., T.G.F. and W.E.H. wrote the main manuscript text and I.R., S.M., A.P., D.B., A.C. and J.G. conducted experiments and prepared figures. All authors reviewed the manuscript.

Additional information

Supplementary information accompanies this paper at http://www.nature.com/scientificreports

Competing financial interests: The authors declare no competing financial interests.

How to cite this article: Raphael, I. *et al.* Microwave & Magnetic (M^2) Proteomics Reveals CNS-Specific Protein Expression Waves that Precede Clinical Symptoms of Experimental Autoimmune Encephalomyelitis. *Sci. Rep.* **4**, 6210; DOI:10.1038/srep06210 (2014).